

## EFFECT OF ANGLE OF ATTACK ON COEFFICIENT OF LIFT OF NACA AIRFOIL BLADE STRUCTURE

K.V.Sreenivas Rao<sup>1</sup> and D.G.Kemparaj<sup>2</sup>

<sup>1</sup>Professor, <sup>2</sup>M.Tech. Student, Department of Mechanical Engineering, Siddaganga Institute of Technology, Tumkur – 572 103, Karnataka, India; email:kvsreenivasarao@yahoo.com

### ABSTRACT

CFD simulations were conducted to estimate the effect of angle of attack on coefficient of lift of NACA 0012 airfoil blade structure. C grid unstructured mesh was generated in Gambit and imported to FLUENT. Simulation of flow field over NACA 0012 Airfoil was successfully completed for subsonic flow case with Mac number  $M=0.3$  & angle of attack  $\alpha=1^0$  to  $8^0$ . The simulated results indicate that the pressure on the lower surface of the airfoil increases while the pressure on the upper surface of the airfoil decreases as the angle of attack increases. The coefficient of lift was found to increase linearly as the angle of attack increases.

**Keywords:** Airfoil, Subsonic flow, Angle of attack, Coefficient of lift

### 1. INTRODUCTION

Flight has been a major part of the world since the Wright brothers first demonstrated it in 1902. In 1915, a committee was formed to accelerate the technology in aviation field known as National Advisory Committee for Aeronautics, henceforth referred to as the NACA, was founded. Scientists at NACA realized that by varying the airfoil geometry, significant improvement in aerodynamic performance could be obtained. [1,2]. A convenient way of describing the aerodynamic characteristics of an airfoil is to plot the values of the coefficients against the angle of attack.

Ramesh V et al, [3] worked on NACA 0012 Airfoil reported a new approach for addition of more points in the region where it is necessary to capture the flow gradients more accurately. N. Gregory And P. G. Wilby [4] concluded that a slightly drooped extension with larger radii of curvature at the leading edge and on the upper surface reduces the maximum velocities in the supersonic region at high Mac numbers and also the strength of the shock wave that terminates it. Marco Turcios [5] compares the results of simulating the Flow Field Around A Joukowski Airfoil Between Theory and experimental data collected at the Parkinson Wind Tunnel at the University of British Columbia. Finally, qualitative comparison was made between FLUENT and OpenFOAM, an open-source CFD package that uses finite volume method. The present work focuses on CFD simulation of flow field around the NACA 0012 airfoil blade structure and presents the effect of angle of attack on pressure variation around the airfoil and the coefficient of lift.

### 2. SCOPE OF THE PRESENT WORK

In the present work C grid domain with structured mesh is generated in Gambit and imported into the FLUENT. The flow field around the airfoil is solved for different test cases, viz; Subsonic, Mac 0.3, for different Angle of Attack ( $\alpha$ )  $0^0$  to  $8^0$  using FLUENT. The coefficient of pressure and coefficient of lift are computed which are in well agreement with the experimental values available from literature survey within NASA Technical Memorandum range for the subsonic

cases. By this process we are able to capture the flow variations around the airfoil very crisply which is clearly shown in contour plots.

### 3. COMPUTATIONAL DOMAIN AND STRATEGY FOLLOWED

The accuracy of CFD solution depends greatly on flow conditions, grid size, and grid quality. The objective of this work is to achieve a high rate of solution using high fidelity commercial CFD solver FLUENT. The Mesh is generated in gambit, a very familiar meshing tool. *.msh* extension file is generated which is imported to FLUENT. The mesh generated is C grid with unstructured mesh domain bounding box (-25 -25 0) (25 25 0). The Mesh is generated with following specification; points: 6864, edges: 23536, faces: 23292, internal faces: 9808, cells: 6864, boundary patches: 3. The generated grid of the computational domain is shown in Figure 1. Solver is set to iterations after getting all the parameters Solver iterations stop as soon as the solution is converged to the predefined residual values For Reynolds number  $3 \times 10^6$  and Mac Number 0.3 coefficient of lift and coefficient of pressure are calculated for different angle of attack and the results are plotted.

### 4. RESULTS AND DISCUSSION

For angle of attack  $\alpha = 0$ , there is no pressure variations on the upper and lower surface of the airfoil. Hence Lift is negligible or no Lift. So pressure contours are not captured.

Figure 2 (a) shows pressure contour for  $M = 0.3$  and  $\alpha = 1^\circ$ . In subsonic flow case, to get the lift the force component acting perpendicular to the free stream velocity in the upper direction should be greater. From the contour plot at leading edge of airfoil at the bottom, a high pressure is obtained compared to upper surface. This satisfies the condition of Lift.

In the Figure 2 (a), at the leading edge of the airfoil, the yellow patch indicates the pressure difference at the lower and upper surface. Here, the maximum patch is towards the lower surface indicating higher pressure. As the pressure and velocity are inversely proportional to each other, the velocity in the lower surface will be low and is indicated in velocity magnitude shown in Figure 2 (b).

The subsequent figures from Figure 2 (c) to Figure 2 (f) show the simulated results of pressure and velocity contours captured for subsonic flow case for  $M = 0.3$  and  $\alpha = 2^\circ$  and  $\alpha = 3^\circ$ . It is evident from the contour plots that the pressure on the lower surface increases with the increase in the angle of attack. This gives rise to increase in the coefficient of lift as the angle of attack increases. This is evident from the pressure coefficient plots shown in Figures 3 (a) (b) and (c).

The Pressure co-efficient plot on the NACA0012 airfoil for the  $M=0.3$  and  $\alpha = 1^\circ$  is shown in figure 3 (a). The upper curve in the graph indicates the upper surface of the airfoil and the lower curve indicates the bottom surface of the airfoil. The point at which both the curves intersect is the Trailing edge pressure recovery. The point at positive values of  $C_p$  is for the leading edge stagnation point of the bottom surface of airfoil indicating higher pressure at the bottom surface. The point at the negative values of  $C_p$ , is for the expansion around leading edge (maximum velocity, first appearance of sonic flow) indicating minimum pressure at the upper surface.

The subsequent figures Figure 3 (b) to Figure 3 (c) show the pressure coefficient for  $M = 0.3$  and  $\alpha = 2^\circ$  and  $\alpha = 3^\circ$ . It is evident from these plots that, as the angle of attack increases, the area under the curve increases indicating higher pressure at the lower surfaces. Hence the maximum lift occurs. The results of the simulated coefficient of lift from  $\alpha = 1^\circ$  to  $8^\circ$  are shown in Figure 3(d). It indicates that the coefficient of lift increases with the increase in the angle of attack. Also, the increase in coefficient of lift is linear with the increase in the angle of attack.

From the coefficient of pressure plots for  $M=0.3$  &  $\alpha=1^\circ$  to  $3^\circ$  it is clear that, as the angle of attack increases, there is an increase in coefficient of pressure positively on the lower surface and negatively on the upper surface of the airfoil. This is due to the variation of pressure on the upper and lower surface of the airfoil. i.e., on the upper surface pressure decreases and on the lower

surface pressure increases. Area under the curve of pressure coefficient plots is increasing as the angle of attack increases. This is because, as the angle of attack increases, projected area on the lower surface of the airfoil increases; hence there is more deviation of particles from the mean path. This change in path is an action and lift of airfoil is reaction. Hence it is obeying Newton's Third law. This is the reason for increase in lift as the angle of attack increases and is shown in the figure 3 (d) for all the cases simulated ( $M=0.3$  &  $\alpha=1^0$  to  $8^0$ ). The contour plots are shown only for three cases, viz;  $M=0.3$  &  $\alpha=1^0$  to  $3^0$

## 5. CONCLUSIONS

Simulation of flow field over NACA 0012 Airfoil using FLUENT was successfully completed for subsonic flow case with  $M=0.3$  & angle of attack  $\alpha=1^0$  to  $8^0$ . C grid unstructured mesh was generated in Gambit and imported to FLUENT. From the simulated results the following conclusions can be drawn.

As the angle of attack increases the difference in pressure on upper and lower surface of airfoil increases. The pressure on the lower surface increases where as the pressure on the upper surface decreases with the increase in the angle of attack. Area under the curve of pressure coefficient plots increases as the angle of attack increases. The coefficient of lift increases as the angle of attack increases. Also, the coefficient of lift increases linearly as the angle of attack increases.

### Figure captions

Fig 1: Grid of Computational Domain

Figure 2 (a): Pressure contours for  $\alpha=1^0$

Figure 2 (b): Velocity Magnitude in m/s for  $\alpha=1^0$

Figure 2 (c): Pressure contours for  $\alpha=2^0$

Figure 2 (d): Velocity Magnitude in m/s for  $\alpha=2^0$

Figure 2 (e): Pressure contours for  $\alpha=3^0$

Figure 2 (f): Velocity magnitude in m/s for  $\alpha=3^0$

Figure 3 (a): Pressure co-efficient plot for  $\alpha = 1^0$

Figure 3 (b): Pressure co-efficient plot for  $\alpha = 2^0$

Figure 3 (c): Pressure co-efficient plot for  $\alpha = 3^0$

Figure 3 (d): Coefficient of Lift Vs Angle of Attack

## REFERENCES

1. Holst, T., and Thomas S.(1933). 'Numerical solution of transonic wing Flow fields' AIAA Journal, 21, 863-70.
2. Holst, T. L., Slooff, J. W., Yoshihara, H., and Ballhaus, W. F. (1982). 'Applied computational transonic aerodynamics.' AGARD AG-266
3. Ramesh, V, .Deshpande, .S.M. & Somasekhar.M from CTFD, of National Aerospace Laboratory, Bangalore India presented a paper on "Point Enrichment For Grid Free Euler Solver"
4. N. Gregory And P. G. Wilby, Ministry Of Defence Aeronautical Research Council Current 'Papers "NPL9615 And NACA0012 A Comparison Of Aerodynamic Data" 1973
5. Marco Turcios, Dr. Kendal Bushe, Department of Mechanical Engineering The University of British Columbia, "Flow over a Joukowski Airfoil Comparison Between Simulation, Experiment and Theory"

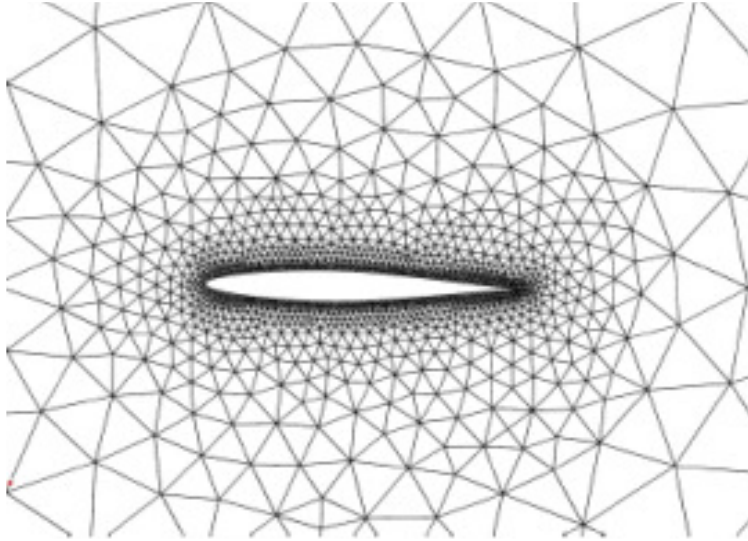


Fig 1: Grid of Computational Domain

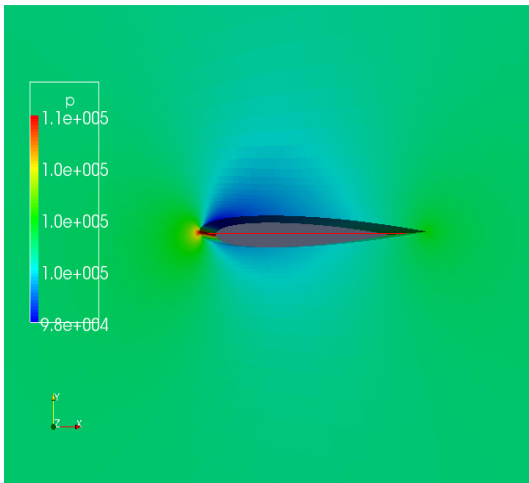


Figure 2 (a): Pressure contours for  $\alpha=1^\circ$

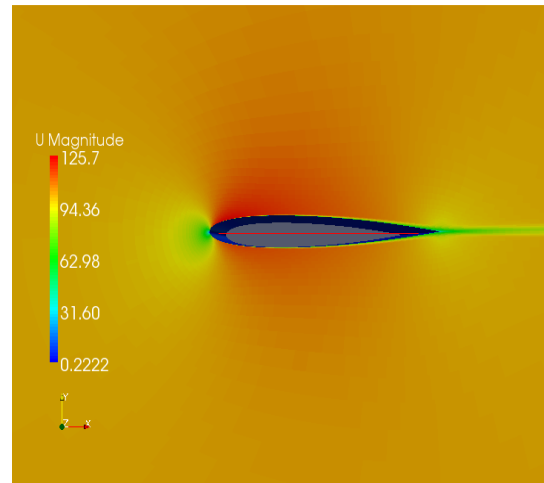


Figure 2 (b): Velocity Magnitude in m/s for  $\alpha=1^\circ$

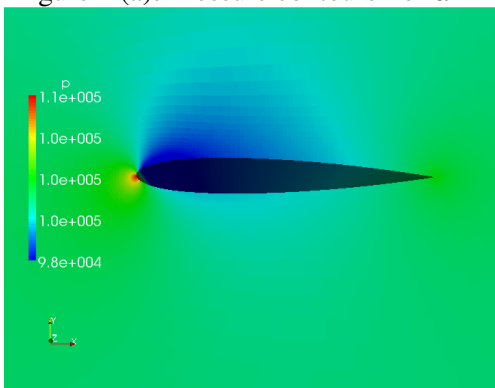


Figure 2 (c): Pressure contours for  $\alpha=2^\circ$

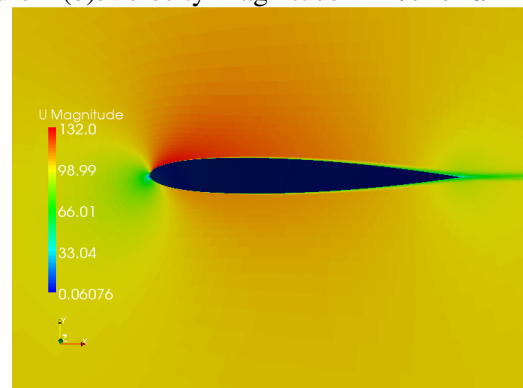


Figure 2 (d): Velocity Magnitude in m/s for  $\alpha=2^\circ$

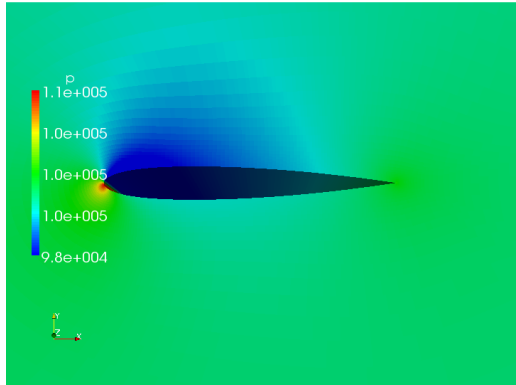


Figure 2 (e): Pressure contours for  $\alpha=3^\circ$

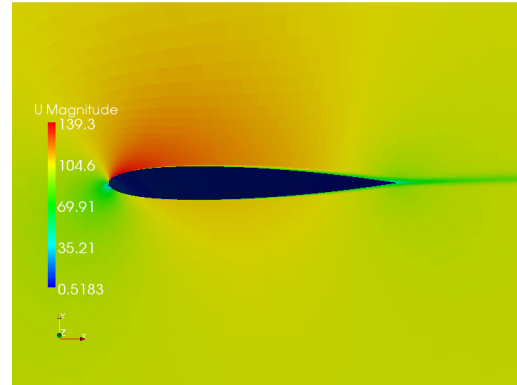


Figure 2 (f): Velocity magnitude in m/s for  $\alpha=3^\circ$

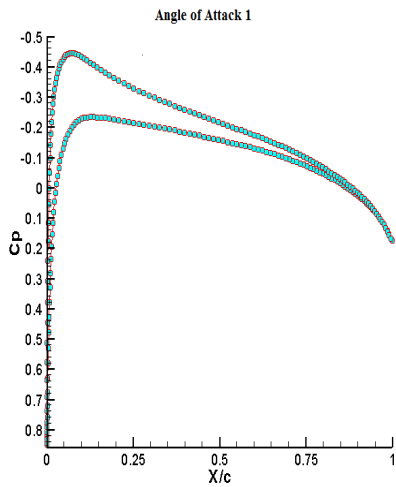


Figure 3 (a): Pressure co-efficient plot for  $\alpha = 1^\circ$

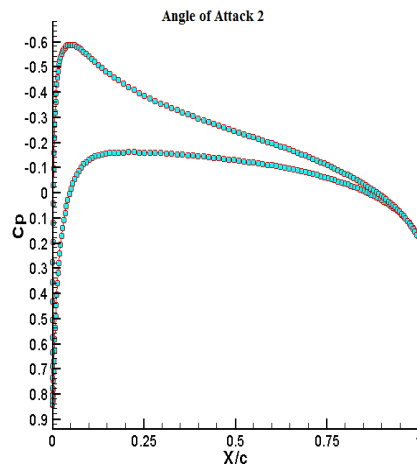


Figure 3 (b): Pressure co-efficient plot for  $\alpha = 2^\circ$

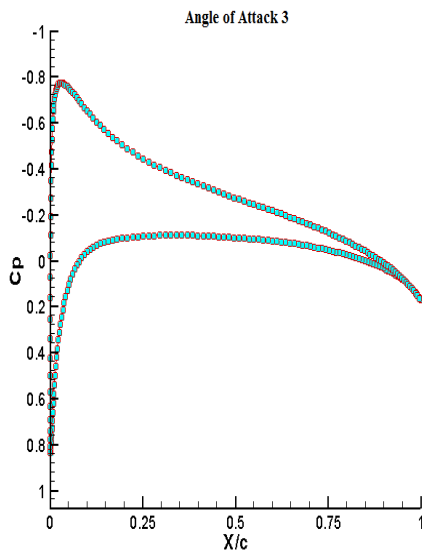


Figure 3 (c): Pressure co-efficient plot for  $\alpha = 3^\circ$

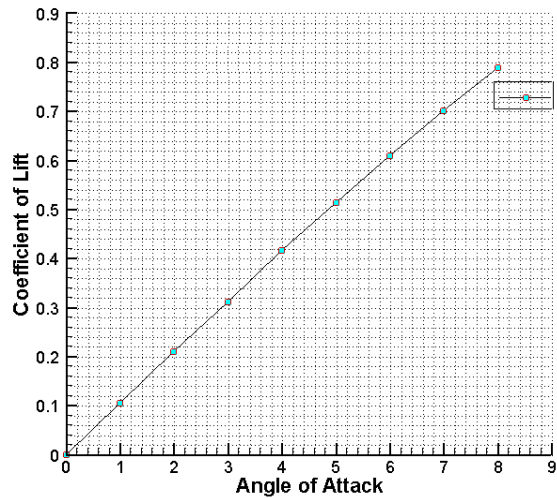


Figure 3 (d): Coefficient of Lift Vs Angle of Attack